REPORT DOCUMENTATION PAGE
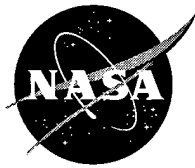
Public reporting burden for this collection of information is estimated to average 1 hour per response, including the time for reviewing instructions, searching existing data sources, gathering and maintaining the data needed, and completing and reviewing the collection of information. Send comments regarding this burden estimate or any other aspect of this collection of information, including suggestions for reducing this burden, to Washington Headquarters Services, Directorate for Information Operations and Reports, 1215 Jefferson Davis Highway, Suite 1204, Arlington, VA 22202-4302, and to the Office of Management and Budget, Paperwork Reduction Project (0704-0188), Washington, DC 20503.

1. AGENCY USE ONLY (Leave blank)	2. REPORT DATE	3. REPORT TYPE AND DATES COVERED
	May 2004	Technical Memorandum

4. TITLE AND SUBTITLE

TF41 Engine Fan Disk Seeded Fault Crack Propagation Test

5. FUNDING NUMBERS

WBS–22–728–30–03
1L162211A47A

6. AUTHOR(S)

David G. Lewicki, William C. Emmerling, Donald Altobelli, Silvia Seng, Chuck Frankenberger, and Leo Fila

7. PERFORMING ORGANIZATION NAME(S) AND ADDRESS(ES)

National Aeronautics and Space Administration
John H. Glenn Research Center at Lewis Field
Cleveland, Ohio 44135–3191

8. PERFORMING ORGANIZATION REPORT NUMBER

E–14567

9. SPONSORING/MONITORING AGENCY NAME(S) AND ADDRESS(ES)

National Aeronautics and Space Administration
Washington, DC 20546–0001
and
U.S. Army Research Laboratory
Adelphi, Maryland 20783–1145

10. SPONSORING/MONITORING AGENCY REPORT NUMBER

NASA TM—2004-213092
ARL–TR–3192

12a. DISTRIBUTION/AVAILABILITY STATEMENT

Unclassified - Unlimited
Subject Category: 37

Distribution: Nonstandard

Available electronically at http://gltrs.grc.nasa.gov

This publication is available from the NASA Center for AeroSpace Information, 301–621–0390.

12b. DISTRIBUTION CODE

13. ABSTRACT (Maximum 200 words)

A cooperative program was conducted between the FAA, U.S. Navy, NASA, and the U.S. Air Force to evaluate crack detection techniques in a seeded fault engine test. The first stage fan of a TF41 engine with a seeded fault was run in a full scale engine test facility. Various disk crack detection systems were installed on the disk and monitored real time. Post-engine-test cycles were accumulated on the TF41 disk in a spin pit to further measure crack growth and disk strain. The crack in the TF41 first stage fan disk grew during the engine test, but significantly less than that predicted from fracture mechanics analysis. Techniques to detect disk crack using center of mass shift seemed feasible in the engine test environment. Techniques to detect disk crack using blade deflections was not effective in this test due to blade wander.

20041008 533

14. SUBJECT TERMS

Crack detection; Engine test; Seeded fault; Vibration; Disk

15. NUMBER OF PAGES

15

16. PRICE CODE

17. SECURITY CLASSIFICATION OF REPORT	18. SECURITY CLASSIFICATION OF THIS PAGE	19. SECURITY CLASSIFICATION OF ABSTRACT	20. LIMITATION OF ABSTRACT
Unclassified	Unclassified	Unclassified	

U.S. ARMY

RESEARCH LABORATORY

TF41 Engine Fan Disk Seeded Fault Crack Propagation Test

David G. Lewicki
U.S. Army Research Laboratory, Glenn Research Center, Cleveland, Ohio

William C. Emmerling and Donald Altobelli
Federal Aviation Administration, William J. Hughes Technical Center, Atlantic City, New Jersey

Silvia Seng and Chuck Frankenberger
Naval Air Warfare Center, Weapons Division, China Lake, California

Leo Fila
Naval Air Systems Command, Patuxent River, Maryland

Since its founding, NASA has been dedicated to the advancement of aeronautics and space science. The NASA Scientific and Technical Information (STI) Program Office plays a key part in helping NASA maintain this important role.

The NASA STI Program Office is operated by Langley Research Center, the Lead Center for NASA's scientific and technical information. The NASA STI Program Office provides access to the NASA STI Database, the largest collection of aeronautical and space science STI in the world. The Program Office is also NASA's institutional mechanism for disseminating the results of its research and development activities. These results are published by NASA in the NASA STI Report Series, which includes the following report types:

- TECHNICAL PUBLICATION. Reports of completed research or a major significant phase of research that present the results of NASA programs and include extensive data or theoretical analysis. Includes compilations of significant scientific and technical data and information deemed to be of continuing reference value. NASA's counterpart of peer-reviewed formal professional papers but has less stringent limitations on manuscript length and extent of graphic presentations.

- TECHNICAL MEMORANDUM. Scientific and technical findings that are preliminary or of specialized interest, e.g., quick release reports, working papers, and bibliographies that contain minimal annotation. Does not contain extensive analysis.

- CONTRACTOR REPORT. Scientific and technical findings by NASA-sponsored contractors and grantees.

- CONFERENCE PUBLICATION. Collected papers from scientific and technical conferences, symposia, seminars, or other meetings sponsored or cosponsored by NASA.

- SPECIAL PUBLICATION. Scientific, technical, or historical information from NASA programs, projects, and missions, often concerned with subjects having substantial public interest.

- TECHNICAL TRANSLATION. English-language translations of foreign scientific and technical material pertinent to NASA's mission.

Specialized services that complement the STI Program Office's diverse offerings include creating custom thesauri, building customized databases, organizing and publishing research results . . . even providing videos.

For more information about the NASA STI Program Office, see the following:

- Access the NASA STI Program Home Page at *http://www.sti.nasa.gov*

- E-mail your question via the Internet to help@sti.nasa.gov

- Fax your question to the NASA Access Help Desk at 301–621–0134

- Telephone the NASA Access Help Desk at 301–621–0390

- Write to:
  NASA Access Help Desk
  NASA Center for AeroSpace Information
  7121 Standard Drive
  Hanover, MD 21076

U.S. ARMY

RESEARCH LABORATORY

TF41 Engine Fan Disk Seeded Fault Crack Propagation Test

David G. Lewicki
U.S. Army Research Laboratory, Glenn Research Center, Cleveland, Ohio

William C. Emmerling and Donald Altobelli
Federal Aviation Administration, William J. Hughes Technical Center, Atlantic City, New Jersey

Silvia Seng and Chuck Frankenberger
Naval Air Warfare Center, Weapons Division, China Lake, California

Leo Fila
Naval Air Systems Command, Patuxent River, Maryland

Acknowledgments

Available from

NASA Center for Aerospace Information
7121 Standard Drive
Hanover, MD 21076

National Technical Information Service
5285 Port Royal Road
Springfield, VA 22100

Available electronically at http://gltrs.grc.nasa.gov

TF41 Engine Fan Disk Seeded Fault Crack Propagation Test

David G. Lewicki
U.S. Army Research Laboratory
National Aeronautics and Space Administration
Glenn Research Center
Cleveland, Ohio 44135
E-mail: david.g.lewicki@grc.nasa.gov

William C. Emmerling and Donald Altobelli
Federal Aviation Administration, William J. Hughes Technical Center
Atlantic City, New Jersey 08405
E-mail: william.emmerling@faa.gov, donald.altobelli@faa.gov

Silvia Seng and Chuck Frankenberger
Naval Air Warfare Center, Weapons Division
China Lake, California 93555
E-mail: silvia.seng@navy.mil, charles.frankenberge@navy.mil

Leo Fila
Naval Air Systems Command
Patuxent River, Maryland 20670
E-mail: filalt@navair.navy.mil

ABSTRACT

A cooperative program was conducted between the FAA, U.S. Navy, NASA, and the U.S. Air Force to evaluate crack detection techniques in a seeded fault engine test. The first stage fan of a TF41 engine with a seeded fault was run in a full scale engine test facility. Various disk crack detection systems were installed on the disk and monitored real time. Post-engine-test cycles were accumulated on the TF41 disk in a spin pit to further measure crack growth and disk strain. The crack in the TF41 first stage fan disk grew during the engine test, but significantly less than that predicted from fracture mechanics analysis. Techniques to detect disk crack using center of mass shift seemed feasible in the engine test environment. Techniques to detect disk crack using blade deflections was not effective in this test due to blade wander.

INTRODUCTION

Although rare in occurrence, a disk rupture in an aircraft engine can lead to a catastrophic failure. In 1989, United Airlines flight 232 crashed during an attempted landing at Sioux Gateway Airport, Iowa [Anon., 1990]. The separation, fragmentation, and forceful discharge of the stage one fan rotor from the number two engine led to leaks in all three hydraulic systems, resulting in loss of flight controls. The failure was due to a fatigue crack in a critical area of the fan disk. Here, 111 fatalities occurred. Another example of a catastrophic disk failure was Delta Air Lines flight 1288 [Anon., 1998]. For this, a crack in the front compressor disk hub propagated to fracture during takeoff roll at Pensacola Regional Airport, Florida. This caused an engine burst where debris penetrated the fuselage. Two passengers were killed and two others were seriously injured. Due to the high speed and high rotational energy in engine disks, cracks in disks can propagate quickly and lead to uncontained engine failures. Techniques to reliably detect disk cracks are extremely important and improvements to these techniques with increased crack detection sensitivity are needed to increase flight safety.

Present day engines are disassembled and disks are inspected using one or more non-destructive evaluation techniques to detect cracks during major overhauls. These techniques are costly, are performed at discrete times during the disk run history, and are not always effective in detecting cracks. Techniques are currently being developed to detect disk cracks during actual operation of the engine. One technique uses vibration monitoring from shaft proximity probes or accelerometers to detect mass imbalance changes caused by rim, bore, or blade cracks [Sonnichsen, 2000; Haase and Drumm, 2002; Rodriguez, et al., 2001]. Another technique uses blade tip sensors measuring blade tip clearance and deflections [Von Flotow, et al., 2000; Dowell, et al., 2000]. These above techniques have shown good success in detecting disk cracks when verified in disk spin pits tests. However, the techniques have not been evaluated in a full scale engine environment. With this in mind, a cooperative U.S. Government program was conducted

between the FAA, U.S. Navy, NASA, and the U.S. Air Force to evaluate crack detection techniques in a seeded fault engine test.

The objective of this paper is to describe the seeded fault engine tests performed to evaluate various engine disk crack detection techniques. The first stage fan of a TF41 engine was chosen as the test specimen. Initially, a finite element method stress analysis and a boundary element method fracture mechanics analysis were performed to give guidance as to size and placement of a seeded defect in the disk. Crack initiation was performed on the TF41 disk with the seeded fault in a spin pit. The disk was then run in a full scale TF41 engine at the U.S. Naval Air Warfare Center China Lake facility. Various disk crack detection systems were installed on the disk and monitored in real time. Lastly, post-engine-test cycles were accumulated on the TF41 disk in a spin pit to further measure crack growth and disk strain. The development of the engine test procedure as well as preliminary results of fault detection techniques are presented.

TEST APPARATUS

Engine Description. The TF41 A-1B engine (Fig. 1a) was chosen as the test article for the seeded fault engine test due to economics (the U.S. Navy had these assets) and prior experience of its fan disk with crack detection techniques. The TF41 engine is an axial flow gas turbine engine with a round fixed geometry inlet, five stage low pressure compressor including a three-stage low bypass ratio fan, and a variable geometry eleven-stage high pressure compressor. The compressor rotors are driven by two-stage low and high pressure turbines through a coaxial shaft. The combustion section consists of ten can-annular axial flow combustors. A bypass duct directs fan discharge air to an annular mixing station which is blended with turbine exhaust gasses upstream of the fixed area convergent exhaust nozzle. The engine has no afterburner. As a result of engine checkout runs, one section of the three-section exhaust nozzle was removed to reduce the engine backpressure and allow higher low-speed shaft (N1) speed. The result of the removal of this section was a 20% increase in the exhaust nozzle area.

The TF41 engine first stage fan (Fig. 1b) was chosen as the test specimen for the crack propagation and detection studies. This was due to its relative ease of visibility for possible external inspections and relative ease of extracting signals from rotating instrumentation. The first stage fan is the first stage of the low pressure compressor. It has dovetailed blades and a slotted disk with a mid-span shroud. The disk material was a titanium forging IMI 679.

Fan Disk/Blade Modeling. Before any tests were performed, extensive modeling was performed on the TF41 engine first stage fan disk. The objective of the modeling was to determine the size and placement of a seeded defect as well
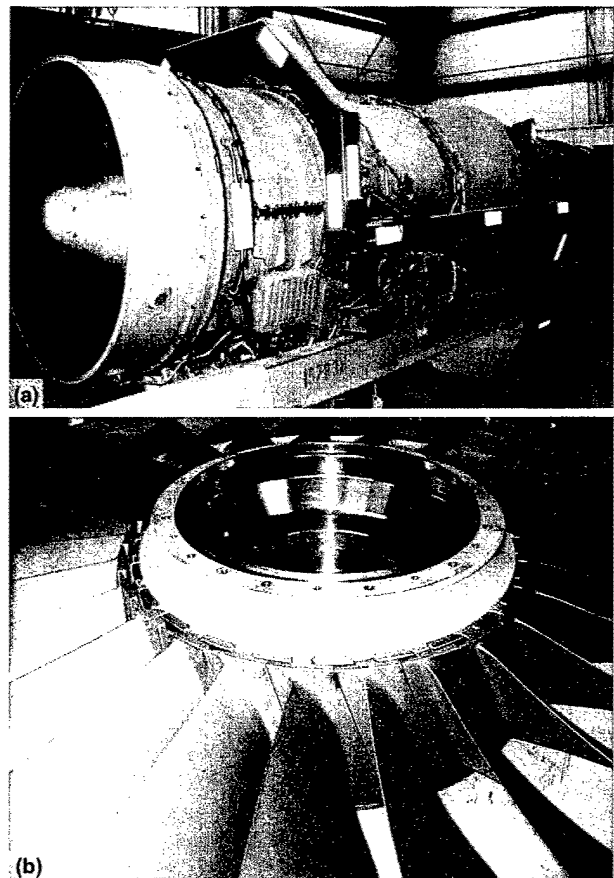

Figure 1. TF41 engine. (a) Full engine view. (b) First stage fan.

as engine run conditions for optimal crack growth. It was desired to grow the largest crack possible for approximately 1500 to 3000 start/stop engine cycles before reaching the disk material's fracture toughness limit and eventual engine disk burst. 3000 cycles was chosen since it would fit into a two-week test run period. Running the engine significantly greater than 3000 cycles was beyond the available time and budget constraints. Running the engine significantly below 1500 cycles would result in too large of a crack growth rate, would prematurely burst the disk, and would limit the crack propagation trending window for diagnostics.

To accomplish optimal crack placement and size, a stress analysis of the TF41 disk/blade using the finite element method (FEM) was first performed [Sarlashkar, et al., 2003]. The finite element model was created by BladePro™, a commercially available turbine blade analysis program which interfaces with the general purpose finite element program ANSYS. A three-dimensional stress analysis was conducted using a single sector model (Fig. 2a). Cyclic boundary conditions were applied. The contact between the blade/disk interface allowed the blade dovetail to slide relative to the dovetail slot in the disk. Explicit contact modeling was not considered at the blade/disk interface and no aerodynamic blade forces were considered. Figure 2b shows the predicted circumferential (hoop) stress distribution through the disk at a speed of 6000 rpm.
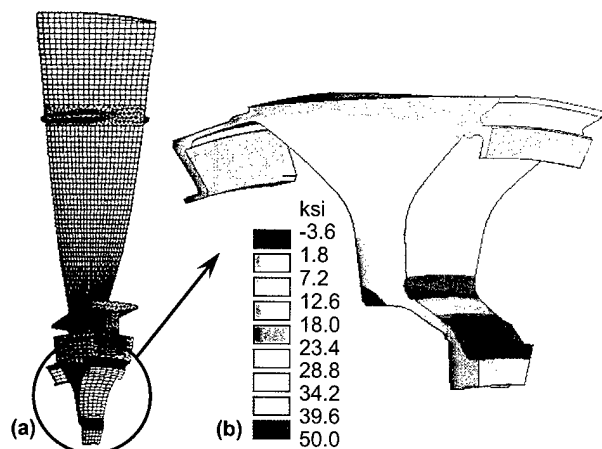
Figure 2. Finite element method stress analysis of TF41 first stage fan disk and blade. (a) Model. (b) Circumferential stress prediction at 6000 rpm.

Once the stress analysis was completed, a fracture mechanics analysis was performed. The FRANC3D crack analysis system [Wawryznek, 1991] was used to determine stress intensity factors for various crack locations and sizes. FRANC3D is based on the boundary element method (BEM) and uses principles of linear elastic fracture mechanics for analysis of cracked structures. An attractive feature of the BEM is that only meshing of the surface of an object is required (especially useful in modeling cracks), unlike FEM where a complete volume mesh is required. A drawback of the BEM is the difficulty in extending the method to include complicated loading conditions and nonlinear analyses, such as the contact conditions at the blade/disk attachments and cyclic symmetry. For the present analyses, these effects were incorporated by means of a superposition principle [Broek, 1986]. This is a well-known technique where stress intensity factors in a cracked structure are computed by applying appropriate tractions to the faces of the crack in an otherwise unloaded structure. Thus, the tractions applied to the crack surfaces in the BEM were derived from the appropriate nodal forces from the FEM analysis. The predicted stress intensity factors versus crack size from the FRANC3D analysis were then imported into a crack growth model to predict number of cycles. The NASGRO crack growth equation [Foreman, et al., 2002] was used. The NASGRO method predicts crack growth rate based on factors such as stress intensity factors, crack closure, fracture toughness, crack threshold, and load ratio. It also requires various material related factors. Unfortunately, the material factors for IMI 679 were not totally available for this study. Some crack growth data for IMI 679 was obtained from the disk material manufacturers, and other NASGRO parameters were deduced by using Ti-6Al-4V titanium factors. This did, however, lead to some uncertainty in the study.

The BEM model used (Fig. 3a) was a 60°-section surface model of the TF41 disk based on a simplified version of the finite element model. In an initial study, three crack locations were considered (Fig. 3b). Locations A and B

were half-penny surface cracks and location C was a corner crack, all on the front side of the disk. The front side was chosen for ease of visibility and ease of instrument installation and wire routing for the engine tests. The cracks were oriented vertically so that the circumferential (hoop) stress due to centrifugal force from disk rotation would be the driving force to grow the crack in engine startup/shutdown low cycle fatigue. Various crack sizes at each location were analyzed. All cracks were either semi-circular (locations A and B) or quarter-circular (location C) with radii from 0.031 to 0.500". Based on FRANC3D stress intensity factors and NASGRO crack growth rates, a trial and error procedure was used to find an initial flaw size that would predict failure in approximately 3000 cyclic load cycles with rpm_{min}=3000 and rpm_{max}=8500. The results showed that the initial crack size, final crack size, and amount of crack growth was larger as you moved away from the disk centerline. Thus, location A was chosen for further studies.

Figure 4 shows the effect of initial crack size and material fracture toughness on predicted crack growth cycles for location A. This was based, as above, with cyclic load cycles of rpm_{min}=3000 and rpm_{max}=8500. For an assumed fracture toughness of K_{IC}=35 ksi√in, an initial crack size of 0.140" gave approximately 3000 cycles to failure. Thus, an initial crack size of 0.140" was the target. Further details of the fracture mechanics analysis are given by Sarlashkar, et al. (2003).
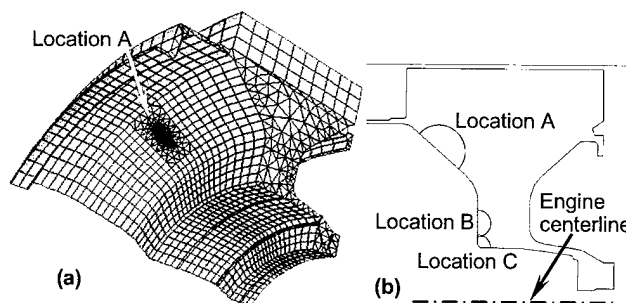

Figure 3. Boundary element method fracture mechanics analysis of TF41 fan disk. (a) Model. (b) Disk cross section with three crack locations investigated.
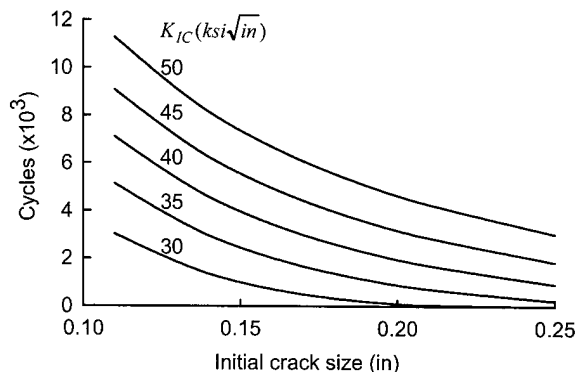

Figure 4. Effect of initial crack size and material fracture toughness property on predicted crack growth.

Disk Crack Initiation Tests. A half-penny shaped semi-circular notch with a radius of 0.100" was machined in the TF41 disk at location A to produce a stress riser and promote crack initiation (Fig. 5). The notch was machined using an electric-discharge machining (EDM) process. In addition, a customized wireless crackwire sensor was fabricated around the notch to monitor crack growth [Gerardi, et al., 2003]. The blades and disk were then assembled and run in a spin pit to initiate a crack. The goal was to produce a crack with radius 0.140" per recommendation from the fracture mechanics analysis. The testing started at cyclic load conditions of rpm_{min}=3000 and rpm_{max}=8500. During spin pit tests, the crackwire system was just used during the first couple days of testing to checkout the system. Also, crack detection using vibration monitoring was rather noisy, making crack detection difficult on-line. Lastly, the installed crackwire physically masked the area around the notch making visual crack detection difficult during routine inspections. With these in mind, a number of different test conditions were run with hopes of initiating a crack (Table I). It was not until 20,138 cycles that crack initiation was confidently suspected. The disk was then inspected using non-destructive evaluation techniques (Brausch, 2003). Eddy current inspection verified the presence of cracks at each end of the EDM notch. The eddy current results indicated each crack to be approximately 0.100 ± 0.010" in length (Fig. 6). Thus, the initial size of the crack was approximately 0.200" in radius, larger than desired from the fracture mechanics analysis. Note that it is extremely difficult, if not impossible, to visually see the crack from the photograph in Fig. 6. That was why eddy current inspection was required. Also, it should be noted that high resolution fluorescent penetrant was ineffective in detecting the crack on the disk surface.
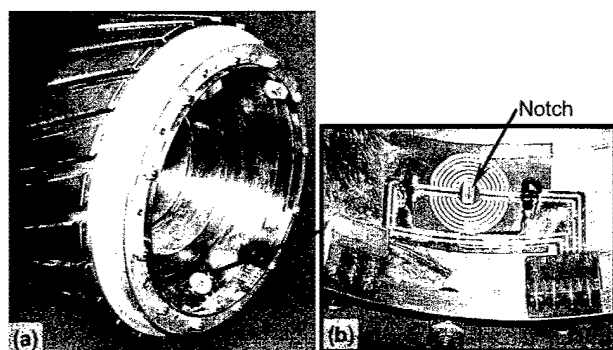
Table I. Run conditions for crack initiation phase in spin pit.

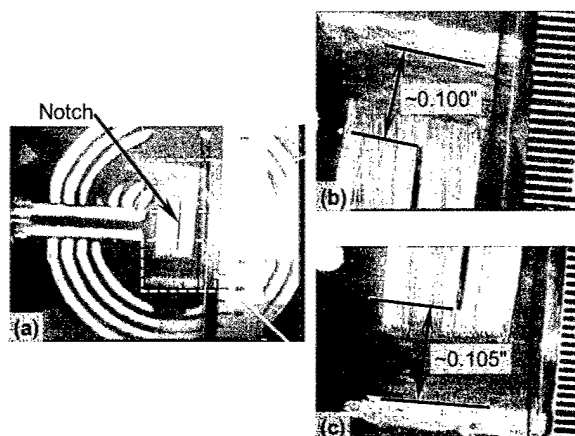|	Total cycles	Min speed (rpm)	Max speed (rpm)
#1	10750	3000	8500
#2	2249	500	8500
#3	1750	3000	8500
#4	999	1500	8500
#5	890	1500	8800
#6	3500	3000	8800
Total	20138		

Figure 6. TF41 first stage fan disk after crack initiation in spin pit. (a) Close-up of notch. (b) Crack growth on inner diameter side. (c) Crack growth on outer diameter side.
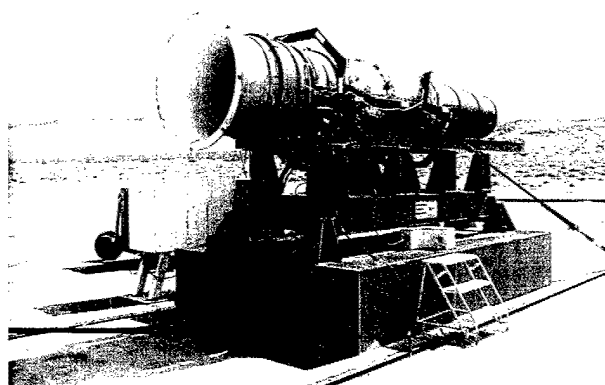

Figure 5. TF41 first stage fan disk. (a) Location of initial notch. (b) Close-up of notch.

Engine Tests. The objective of the engine tests was to demonstrate crack detection technologies in an actual engine environment. The approach taken was to: (1) install the TF41 engine (with the seeded fault first stage disk consisting of a 0.200" radius semi-circular crack) in an engine test facility, (2) install various real-time crack detection techniques on the engine, (3) cycle the engine through idle/max sequences to promote crack propagation through

Figure 7. U.S. Navy China Lake engine test facility.

low cycle fatigue, (4) continue cycles until disk rupture / engine burst or schedule completion occurred. The tests were performed at the U.S. Naval Air Warfare Center, Weapons Survivability Lab, China Lake, CA (Fig. 7). Seven participating companies with various Government contracts with the FAA, U.S. Navy, NASA, and U.S. Air Force were involved in the crack detection tests. The following crack detection technologies were evaluated:
• vibration monitoring, shaft position monitoring, fan blade position monitoring, and appropriate algorithms to detect mass imbalance due to a disk crack

- fan blade clearance and timing monitoring and appropriate algorithms to determine blade and disk deformation and disk crack growth
- acoustic emission monitoring to detect a disk crack
- disk rotation monitoring using optical encoders to determine torsional resonances and changes due to disk crack growth
- wireless, crackwire coating on the disk to monitor crack size and growth

Instrumentation. A diagram of the stationary sensors installed on the TF41 engine for crack detection is given in Fig. 8. An instrumentation ring was mounted on the plate seal of the stator aft of the first stage fan. The ring was tack-welded to the bolt circle on the front static air seal. The instrumentation ring contained radial proximity probes for disk shaft position and speed sensors for order tracking. The sensor wires were routed outside the engine case through hollow stator vanes. A number of eddy current sensors and capacitive sensors were mounted on or through the fan case for blade tip timing and blade tip clearance measurements. A number of accelerometers were mounted on the fan and compressor cases to measure engine vibration. Two fiber optic sensors were mounted near the instrumentation ring to measure disk torsional resonance. In addition to the stationary sensors, two rotating acoustic emission sensors were mounted on the fan disk itself. Also, a crackwire sensor was fabricated around the notch of the fan disk to measure crack growth. Both the acoustic emission sensors and crackwire sensor shared a common radio frequency (RF) telemetry system fabricated for this test. An armored instrumentation box was located on the test pad near the engine containing appropriate signal conditioning electronics for the above instrumentation. The output signals were then run to the control room located approximately 700 ft from the engine test pad.

In addition to the crack detection instrumentation, facility instrumentation for general engine operating conditions consisted of low and high pressure rotor speeds, power level angle, engine oil pressure, exhaust pressure, turbine exit temperature, fuel flow, atmospheric pressure, and ambient air and fuel temperatures. Also, a number of video cameras as well as high-speed digital cameras were used to monitor and record the response of the test engine and were prepared to capture disk burst photography.

RESULTS AND DISCUSSION

Engine Test Results. Engine checkout runs on an uncracked first stage fan disk were performed prior to the seeded fault test to ensure nominal engine performance and test stand functionality. For the seeded fault test, the engine was run for a repeated number of throttle power cycles. The engine was run approximately nine to ten hours per day when possible for a two-week period. The various crack detection methods were monitored real-time during the test. After the
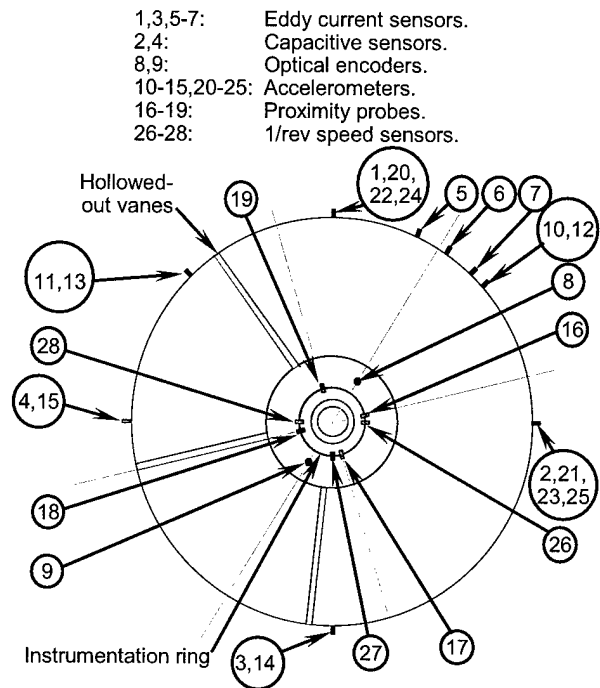
1,3,5-7:   Eddy current sensors.
2,4:   Capacitive sensors.
8,9:   Optical encoders.
10-15,20-25: Accelerometers.
16-19:   Proximity probes.
26-28:   1/rev speed sensors.

Figure 8. Instrumentation installed on TF41 engine (front view of engine with first stage fan disk removed).
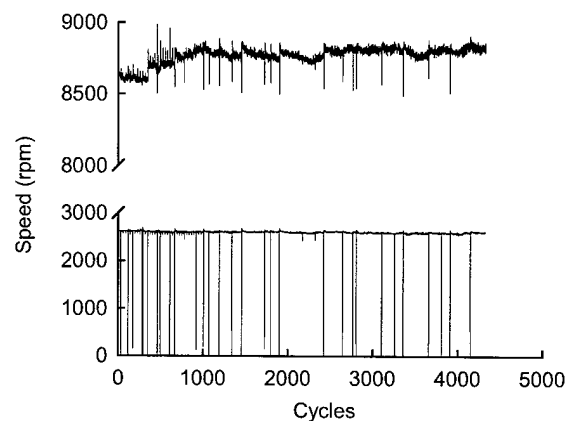

Figure 9. TF41 engine test run conditions.

two week period, the disk did not rupture and the crack detection techniques did not give clear indication of significant crack growth. The fan endured a total of 4,474 on-engine throttle power cycles. Figure 9 plots the maximum and idle speeds for the power cycles.

For the throttle power cycles, a throttle cable was installed on the engine throttle controls. A step motor was placed on the engine stand to allow the throttle to be actuated from the control room. A computer program provided the acceleration/deceleration schedule. The throttle control worked by advancing the throttles to the maximum power level setting and controlling the engine speed using the airflow limiter. The engine T2 sensor was fed a false temperature signal to take advantage of the TF41 airflow limiter restricting the speed to the desired maximum N1 rpm for testing. This method, however, did produce some
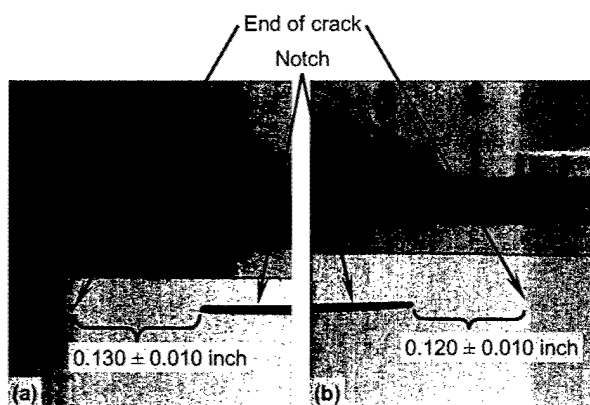
Figure 10. TF41 first stage fan disk after engine test. (a) Crack growth on outer diameter side. (b) Crack growth on inner diameter side.

Figure 11. TF41 engine test crack detection using mass imbalance techniques. (a) Mass imbalance. (b) Crack induced imbalance.

Figure 12. TF41 engine test crack detection using mass imbalance techniques.

variability of the resulting speed. Also, note that the maximum speed set point was increased at cycle 285. The maximum speed at the start of the test was set for 8500 rpm due to concern that the crack would grow too quickly based on the fracture mechanics predictions and initial crack size from the spin pit tests. The maximum speed was then increased to 8800 rpm when the crack did not grow as fast as expected. Specific details of the test are given by Seng (2004).

At the conclusion of the test, the fan and blades were removed from the engine and inspected. Eddy current inspection revealed a crack length of 0.130 ± 0.010" beyond the EDM notch on the outer diameter side of the notch and 0.120 ± 0.010" beyond the notch on the inner diameter side (Fig. 10). Thus, the crack grew approximately 0.020 to 0.025" during the seeded fault engine test. The fracture mechanics analysis predicted crack growth of 0.2" and eventual disk burst for 4,474 cycles. Thus, the actual crack growth from the engine tests was far less than the predicted amount of crack growth from the fracture mechanics analysis. Again, as with Fig. 6, it is extremely difficult, if not impossible, to visually see the crack from the photograph in Fig. 10.

Crack Detection Evaluation. Results for one vibration based crack detection technique are given in Fig. 11 (Luo, et al., 2004). Here, vibrations from accelerometers mounted on the fan case are processed. A non-resonant synchronous vibration based detection algorithm was developed for operational speeds between two consecutive natural frequencies of a multi-degree of freedom rotor machinery. Series expansions of predicted responses lead to classifying vibration due to mass imbalance and crack induced imbalance based on series coefficients. As seen from the figure, a general upward trend of imbalance is shown as cycles increase. However, there is much noise in the data. Also, the increase in mass imbalance is almost as large as the increase in crack induced imbalance. Thus, no significant crack growth could be deduced from the method.
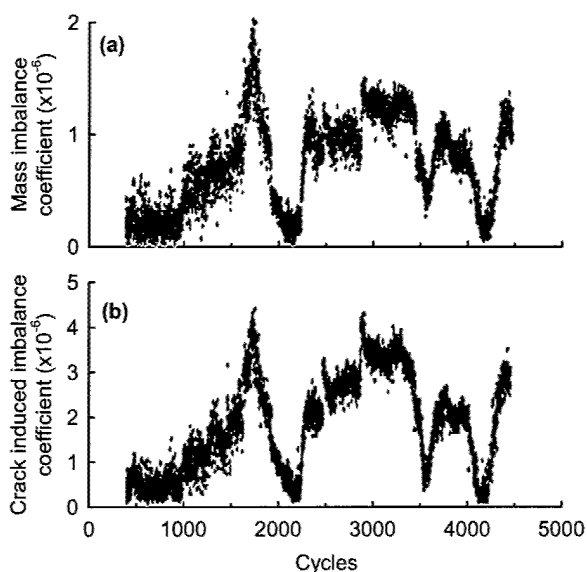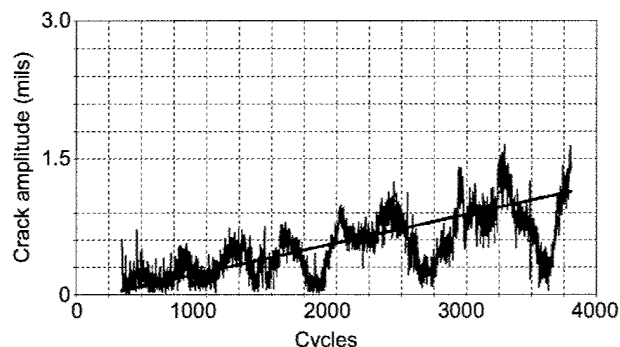
A second methodology, also based on crack induced mass imbalance, is given in Fig. 12. Here, vibration from disk shaft proximity probes is processed by the method given by Sonnichsen (2000). The vibration signal is processed through a proprietary tracking filter, and the synchronous amplitude and phase angle are measured. From the figure, a general increasing trend in crack amplitude is shown as cycles increase. However, the signal is still rather noisy and definitive crack growth prediction is questionable.

A third methodology, also based on crack induced mass imbalance, is given in Fig. 13. Here, blade tip radial clearance from a capacitive sensor is processed by the method given by Haase and Drumm (2002). The magnitude and phase of the change in mass center had a significant increase at cycle 3200, but dropped back to nominal after, again showing difficulty in definitive crack detection.

The above techniques for crack detection based on change of mass imbalance had difficulties in giving significant indication of crack growth during the TF41 tests. This may have been due to the relatively small amount of crack
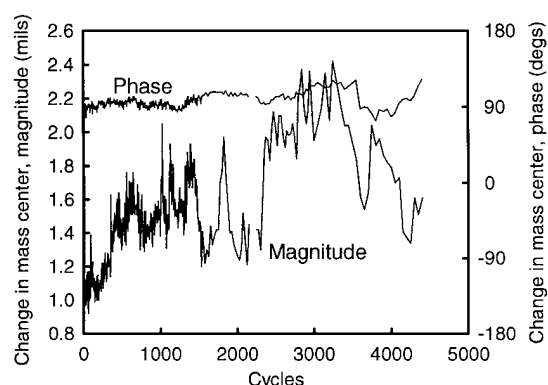
Figure 13. TF41 engine test crack detection using mass imbalance techniques.
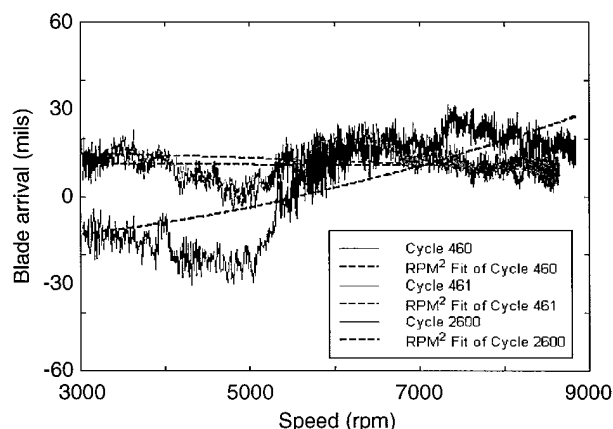

Figure 14. Blade position as a function of speed; TF41 engine test crack detection using blade tip deflection.

growth for the engine tests (0.020 to 0.025"), and the change in signal responses due to crack growth may have been buried in the nominal noise. Also, it is suspected that the engine was approaching a resonant frequency near the maximum speed tested, thus complicating the vibration and masking the sensitivity of the techniques. An encouraging trend, however, was that most did give some type of increased response with increased cycles.

Figure 14 shows the results from the blade deflection measurements. Previous studies have shown that the calculated blade arrival time based on blade tip deflection measurements can be a good indicator of potential cracks. For the TF41 tests, the blades drifted considerably in the tangential position over a large number of cycles. It is believed that this drift was mechanical axial drift along the contact surfaces of the mid-span snubbers. It is not clear why the blades drifted back and forth and did not find a favored position. Regardless, the drift prevented this technique from detecting the small crack growth during the engine tests.

Initial results from the wireless, crackwire coating were intermittent due to electrical connection problems. Once corrected, the crackwire performed reasonably well for the tests. Near completion of the engine test, all crackwires read

intact at idle after 4,474 cycles. The sensor grid inner crackwire opened at 7000 rpm (inner crackwire 0.060 to 0.090" from the notch tip). For the remaining sensors, the results from the acoustic emission sensors were inconclusive due to amplifier saturation in the telemetry system. Lastly, the results from the optical encoder sensors were inconclusive due to instrumentation problems and blade drift.

Post Engine Test Studies. Follow-on tests were performed on the TF41 first stage fan disk to give further insight for the discrepancy between predicted and measured crack growth during the engine test. The TF41 fan disk was instrumented with two crack propagation gages from Lewicki (1995) and six conventional strain gages (Fig. 15). The two crack propagation gages were placed on both sides of the notch tip at a distance of 0.100" (note that this overlapped the measured crack from the latest eddy current inspection). Two strain gages were placed, one on each side of the EDM notch, at a distance of 1.50" and at the same radial position of the notch center. Two additional strain gages were placed at the same positions, but rotated 180° about the disk centerline. Lastly, two gages were placed like the first two, but on the aft side of the disk. The blades and disks were assembled and run in a spin pit. The objectives of the test were to: (1) measure crack growth rates in the spin pit, and (2) measure strain on the disk for comparisons to the FEM predictions and future engine tests.

The measured strains for the six strain gages from the first cycle in the spin pit are given in Table II. These measurements are for a disk speed of 8800 rpm. The strain measurement locations were on the same radius of the disk and it was expected that the strains would be similar for these locations. This was pretty much the case as the measured strain were within 5% of the average. Also, the measured strain was in good correlation with the FEM predictions. The FEM calculated strain was about 7% higher than the measured.
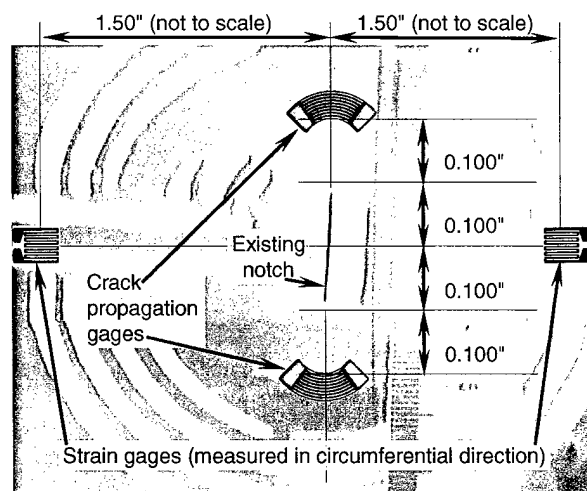

Figure 15. Instrumentation for post engine test follow-on studies.

Table II. Strain measurements of TF41 disk at 8800 rpm.

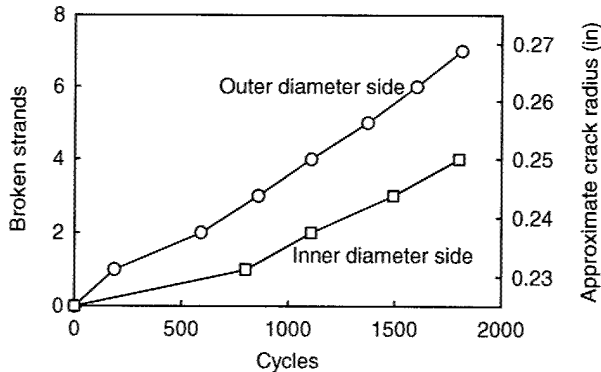| Location	Strain ($\mu\varepsilon$)
Upstream, +1.50" from crack	3455
Upstream, -1.50" from crack	3262
Upstream, 180 deg, +1.50" from crack	3345
Upstream, 180 deg, -1.50" from crack	3571
Downstream, +1.50" from crack	3578
Downstream, -1.50" from crack	3484

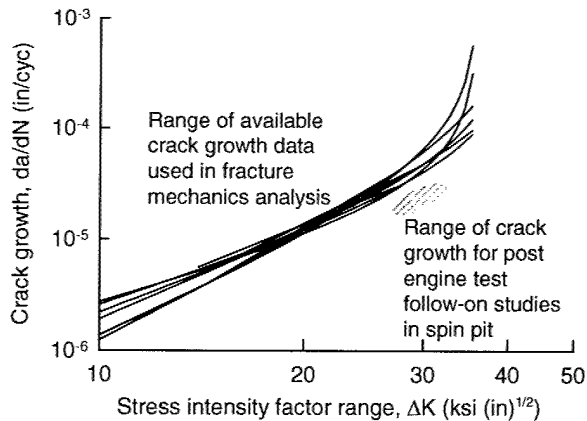**Figure 16.** Crack propagation for post engine test follow-on studies in spin pit.

Figure 17. Comparison of crack growth post engine test follow-on studies in spin pit to available material data for IMI 679.

Figure 16 gives the results from the crack propagation gages for the spin pit test. A total of 1,812 cycles were accumulated on the disk for cyclic load conditions of rpm_{min}=2800 and rpm_{max}=8800. Seven strands broke for the gage on the outer diameter side of the notch and four broke for the gage on the inner diameter side. This gave approximately 0.027 to 0.047" in crack growth. For the 1,812 cycles, this resulted in crack growth rates of 1.5 to 2.5 x 10^{-5} in/cyc. Figure 17 plots the crack growth rates for the post engine test studies compared to rates from material characterization data used in the fracture mechanics analysis.

Again, the material data used in the fracture mechanics came from a number of sources, were rather sparse in content, and had some variation between them. As seen in the figure, the measured crack growth from the post engine test studies was noticeably lower than the material data.

As stated before, the crack grew approximately 0.020 to 0.025" for the 4,474 cycles of the seeded fault engine test. This resulted in crack growth rates of 4.5 to 5.6 x 10^{-6} in/cyc. Thus, the measured crack growth from the China Lake engine tests was approximately four time less than the growth from the post engine test studies. The reason for the lower crack growth in the engine test is currently under investigation. Some leading causes could be improper material characterization in the fracture mechanics model, a reduction in stress due to aerodynamic or thermal loads in the engine test, residual stress in the disk, variability in maximum power conditions in the engine test, occasional overloads in the engine test leading to crack arrest, or other causes.

CONCLUSIONS

A cooperative program was conducted between the FAA, U.S. Navy, NASA, and the U.S. Air Force to evaluate crack detection techniques in a seeded fault engine test. The first stage fan of a TF41 engine was run in a full scale engine facility. Various disk crack detection systems were installed on the disk and monitored real time. Post-engine test cycles were accumulated on the TF41 disk in a spin pit to further measure crack growth and disk strain. The following results were obtained:

1) The crack in the TF41 first stage fan disk grew 0.100" in radius from a seeded notch in spin pit tests. The crack then grew approximately 0.020 to 0.025" in radius during the engine test, but was significantly less than that predicted from fracture mechanics analysis.

2) Techniques to detect a disk crack using center of mass shift seemed feasible in the actual engine test environment, but did not prove to give definitive results for the relatively small amount of crack growth from the engine test. Techniques to detect a disk crack using blade deflections were not effective in this test due to blade wander.

3) The measured strain in the TF41 first stage fan disk from spin pit tests correlated well with finite element method predictions. The measured crack growth from the post engine test studies was noticeably lower than the crack growth rate from previous material tests. The measured crack growth from the China Lake engine test was approximately four time less than the growth from the post engine test studies in a spin pit at similar run conditions.

REFERENCES

Anon., "United Airlines Flight 232. McDonnell Douglas DC-10-10, Sioux Gateway Airport, Sioux City, Iowa, July 19, 1989", National Transportation Safety Board Report No. NSTB/AAR-90/06, Nov. 1990.

Anon., "Uncontained Engine Failure, Delta Air Lines Flight 1288, McDonnell Douglas MD-88, N927DA, Pensacola, Florida, July 6, 1996", National Transportation Safety Board Report No. NSTB/AAR-98/01, Jan. 1998.

Brausch, J.C., "TF-41 Test Rotor (Nondestructive Evaluation)", Wright-Patterson Air Force Base Report No. AFRL/MLS 03-024, Mar. 2003.

Broek, D., "Elementary Engineering Fracture Mechanics", 4th Edition, Martinus Nijhoff, Dordrecht, 1986.

Dowell, M., et al., "Progress in Turbomachinery Prognostics and Health Management via Eddy-Current Sensing", Aerospace Conference Proceedings, 2000 IEEE, Vol. 6, pp. 133-143, 2000.

Foreman, R.G., et al., "NASGRO, Fracture Mechanics and Fatigue Crack Growth Analysis Software, Reference Manual, Version 4.02, Sep. 2002.

Gerardi, J.J., Archambault, J., and Brooks, W.G., "Wireless Crackwire Sensor for In-Situ Engine Monitoring", Aerospace Conference, 2003 Proceedings, 2003 IEEE, Vol. 7, pp. 7-3045 - 7-3052, 2003.

Haase, W., and Drumm, M.J., "Detection, Discrimination and Real-Time Tracking of Cracks in Rotating Disks", Aerospace Conference Proceedings, 2002 IEEE, Vol. 6, pp. 6-3095 - 6-3104, 2002.

Lewicki, D.G., "Crack Propagation Studies to Determine Benign or Catastrophic Failure Modes for Aerospace Thin-Rim Gears", Ph.D. Dissertation, Case Western Reserve University, May 1995 (also NASA TM-107170, Army Research Laboratory Report ARL-TR-971, May 1996).

Luo, H., Rodriguez, H., and Hallman, D., "Disk Crack Detection for Seeded Fault Engine Test", NASA Contractor Report in progress, Contract No. NAS 3-01135, Task Order 7, 2004.

Rodriguez, H.M., Hallman, D., and Butz, M., "A Physics-Based Approach for the Detection of Cracks in Rotating Disks", presented at the XV ISABE 15th International Symposium on Airbreathing Engines, Bangalore, India, Sep. 2001.

Sarlashkar, A.V., et al., "Model-Based Analysis in Support of the TF-41 Seeded-Fault Testing", Aerospace Conference, 2003 Proceedings, 2003 IEEE, Vol. 7, pp. 7-3033 - 7-3044, 2003.

Seng, S., "Fan Disk Crack Detection Test Report", U.S. Department of Transportation, Federal Aviation Administration report in progress, Contract No. DTFA03-01-X-90013, 2004.

Sonnichsen, H.E., "Real-time Detection of Developing Cracks in Jet Engine Rotors", Aerospace Conference Proceedings, 2000 IEEE, Vol. 6, pp. 173-183, 2000.

Von Flotow, A., Mercadal, M., and Tappert, P., "Health Monitoring and Prognostics of Blade and Disks with Blade Tip Sensors", Aerospace Conference Proceedings, 2000 IEEE, Vol. 6, pp. 433-440, 2000.

Wawrzynek, P.A., Discrete Modeling of Crack Propagation: Theoretical Aspects and Implementation Issues in Two and Three Dimensions, Ph.D. Thesis, Cornell University, Aug. 1991.